HIGGS BOSON PRODUCTION IN e^+e^- AND e^-e^- COLLISIONS*

PER OSLAND

Department of Physics, University of Bergen
Allégaten 55, N-5007 Bergen, Norway

(Received March 8, 1999)

When Higgs boson candidates will be found at future colliders, it becomes imperative to determine their properties, beyond the mass, production cross section and decay rates. Other crucial properties are those related to the behaviour under CP transformations, and the self-couplings. This paper addresses the question of measurability of some of the trilinear couplings of MSSM neutral Higgs bosons at a high-energy e^+e^- collider, and the possibilities of exploring the Higgs boson CP properties at e^+e^- and e^-e^- colliders.

PACS numbers: 14.80.Cp, 12.60.Jv, 13.90.+i

Dedicated to the memory of Bjørn Håvard Wiik

1. Introduction

The Higgs particle is expected to be discovered at the LHC, if not already at LEP [1]. Current estimates from precision electroweak data [2] suggest that it is rather light. A light Higgs particle would be consistent with both the Standard Model (SM) and the Minimal Supersymmetric Standard Model (MSSM). A detailed measurement of its branching ratios should enable one to distinguish between these two most favoured models.

However, there is more to the MSSM Higgs sector than branching ratios. For a complete analysis, one should also measure the trilinear and quartic self-couplings, which in the MSSM are determined by the gauge couplings.

The measurability of couplings involving the light Higgs particle was investigated by Djouadi, Haber and Zerwas [3]. It was concluded that the

* Presented at the Cracow Epiphany Conference on Electron–Positron Colliders, Cracow, Poland, January 5–10, 1999.

trilinear couplings λ_{Hhh} and λ_{hhh}, where h and H denote the two neutral, CP-even Higgs bosons, could be measured at a high-energy linear collider. This early study neglected squark mixing, but, with some limitations, the conclusion was confirmed also for the case of squark mixing [4]. A recent study also accounts for the dominant two-loop effects [5].

One should keep in mind that the Higgs sector might be more rich than suggested by the MSSM [6]. Thus, it would be most useful to establish the CP properties of the Higgs particle from basic principles. A straightforward method to determine the parity is to study the angular distribution of the Higgs particle itself [7,8]. A second approach makes use of the orientation of the plane spanned by the fermions from the accompanying Z boson in the Bjorken process [9–11].

We also review the production of scalar Higgs-like particles in high-energy electron–electron collisions, via the fusion of electroweak gauge bosons. The emphasis is on how to distinguish a CP-even from a CP-odd Higgs particle [12]. Among the more significant differences, we find that in the CP-odd case, the Higgs spectrum is much harder, and the dependence of the total cross section on the product of the polarizations of the two beams is much stronger, as compared with the CP-even case. We also briefly discuss parity violation, and the production of charged Higgs bosons.

2. Trilinear Higgs couplings

Trilinear couplings of the neutral CP-even Higgs bosons in the Minimal Supersymmetric Standard Model (MSSM) can be measured through the multiple production of the lightest CP-even Higgs boson at high-energy e^+e^- colliders. The relevant production mechanisms are the production of the heavier CP-even Higgs boson via $e^+e^- \to ZH$, in association with the CP-odd Higgs boson (A) in $e^+e^- \to AH$, or via the fusion process $e^+e^- \to \nu_e\bar{\nu}_e H$, with H subsequently decaying through $H \to hh$.

The trilinear Higgs couplings that are of interest are λ_{Hhh}, λ_{hhh}, and λ_{hAA}, involving both the CP-even and CP-odd Higgs bosons. The couplings λ_{Hhh} and λ_{hhh} are rather small with respect to the corresponding trilinear coupling $\lambda^{\rm SM}_{hhh}$ in the SM (for a given mass of the lightest Higgs boson m_h), unless m_h is close to the upper value (decoupling limit). The coupling λ_{hAA} remains small for all parameters.

We have considered the question of possible measurements of the trilinear Higgs couplings λ_{Hhh} and λ_{hhh} [4] of the MSSM [13] at a high-energy e^+e^- linear collider that will operate at an energy of 500 GeV with an integrated luminosity per year of $\mathcal{L}_{\rm int} = 500\,{\rm fb}^{-1}$ [14]. In a later phase one may envisage an upgrade to an energy of 1.5 TeV.

The multiple production of the light Higgs boson through Higgsstrahlung of H, and through production of H in association with the CP-odd Higgs boson can be used to extract the trilinear Higgs coupling λ_{Hhh}. The non-resonant fusion mechanism for multiple h production, $e^+e^- \to \nu_e\bar{\nu}_e hh$, involves two trilinear Higgs couplings, λ_{Hhh} and λ_{hhh}, and is useful for extracting λ_{hhh}.

In units of $gm_Z/(2\cos\theta_W) = (\sqrt{2}G_F)^{1/2}m_Z^2$, the *tree-level* trilinear Higgs couplings involving h are given by

$$\lambda^0_{Hhh} = 2\sin 2\alpha \sin(\beta+\alpha) - \cos 2\alpha \cos(\beta+\alpha), \quad (1)$$

$$\lambda^0_{hhh} = 3\cos 2\alpha \sin(\beta+\alpha), \quad (2)$$

$$\lambda^0_{hAA} = \cos 2\beta \sin(\beta+\alpha), \quad (3)$$

with α the mixing angle in the CP-even Higgs sector, which is determined by the parameters of the CP-even Higgs mass matrix.

We include one-loop radiative corrections [15, 16] to the Higgs sector in the effective potential approximation. In particular, we take into account [4] the parameters A and μ, the soft supersymmetry breaking trilinear parameter and the bilinear Higgs(ino) parameter in the superpotential. These parameters enter through the stop masses,

$$m^2_{\tilde{t}_{1,2}} = m_t^2 + \tilde{m}^2 \pm m_t(A + \mu\cot\beta) \quad (4)$$

which again enter through the radiative corrections to the Higgs masses as well as to the Higgs trilinear couplings. The dominant one-loop radiative corrections are proportional to $(m_t/m_W)^4$, multiplying functions depending on the squark masses [15, 16].

The trilinear couplings depend significantly on m_A, and thus also on m_h. This is shown in Fig. 1, where we compare λ_{Hhh}, λ_{hhh} and λ_{hAA} for three different values of $\tan\beta$, and the SM quartic coupling $\lambda^{\rm SM}$ (which also includes one-loop radiative corrections [17]). For a given value of m_h, the values of these couplings significantly depend on the soft supersymmetry-breaking trilinear parameter A, as well as on μ.

As is clear from Fig. 1, at low values of m_h, the MSSM trilinear couplings are rather small. For some value of m_h the couplings λ_{Hhh} and λ_{hhh} start to increase in magnitude, whereas λ_{hAA} remains small. The values of m_h at which they start becoming significant depend crucially on $\tan\beta$.

To sum up the behaviour of the trilinear couplings, we note that λ_{Hhh} and λ_{hhh} are small for $m_h \lesssim$ 100–120 GeV, depending on the value of $\tan\beta$. However, as m_h approaches its maximum value, which requires $m_A \gtrsim 200$ GeV, these trilinear couplings become reasonably large.

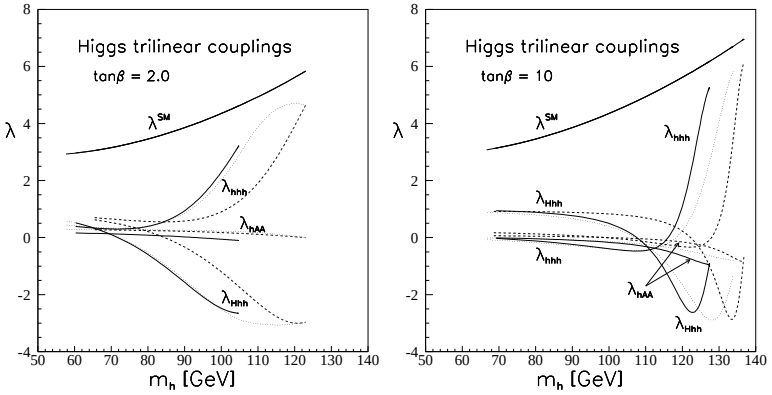

Fig. 1. Trilinear Higgs couplings λ_{Hhh}, λ_{hhh} and λ_{hAA} as functions of m_h for $\tan\beta = 2.0$ and $\tan\beta = 10.0$. Each coupling is shown for $\tilde{m} = 1$ TeV, and for three cases of the mixing parameters: no mixing ($A = 0$, $\mu = 0$, solid), mixing with $A = 1$ TeV and $\mu = -1$ TeV (dotted), as well as $A = 1$ TeV and $\mu = 1$ TeV (dashed).

3. Production mechanisms

Different mechanisms for multiple production of the MSSM Higgs bosons in e^+e^- collisions have been discussed by DHZ [3]. The dominant mechanism for the production of multiple CP-even light Higgs bosons is through the mechanisms

$$\left.\begin{array}{lcl} e^+e^- & \to & ZH, AH \\ e^+e^- & \to & \nu_e\bar{\nu}_e H \end{array}\right\}, \qquad H \to hh, \tag{5}$$

shown in Fig. 2. The heavy Higgs boson H can be produced by H-strahlung, in association with A, and by the resonant WW fusion mechanism. All the diagrams of Fig. 2 involve the trilinear coupling λ_{Hhh}.

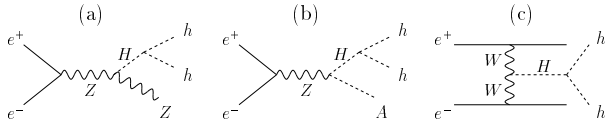

Fig. 2. Feynman diagrams for the resonant production of hh final states in e^+e^- collisions.

A background to (5) comes from the production of the pseudoscalar A in association with h and its subsequent decay to hZ

$$e^+e^- \to hA, \qquad A \to hZ, \tag{6}$$

leading to Zhh final states. A further mechanism for hh production is double Higgs-strahlung in the continuum with a Z boson in the final state,

$$e^+e^- \to Z^* \to Zhh. \tag{7}$$

There is also a mechanism of multiple production of the lightest Higgs boson through non-resonant WW fusion in the continuum:

$$e^+e^- \to \bar{\nu}_e\nu_e W^*W^* \to \bar{\nu}_e\nu_e hh, \tag{8}$$

as shown in Fig. 3.

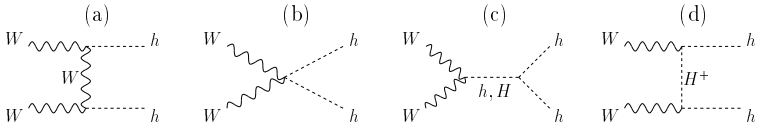

Fig. 3. Feynman diagrams for the non-resonant WW fusion mechanism for the production of hh states in e^+e^- collisions.

It is important to note that all the diagrams of Fig. 2 involve the trilinear coupling λ_{Hhh} only. In contrast, the non-resonant analogues of Figs 2(a), 2(b) and 2(c) (or 3(c)) involve both the trilinear Higgs couplings λ_{Hhh} and λ_{hhh}.

3.1. Higgs-strahlung and associated production of H

The dominant source for the production of multiple light Higgs bosons in e^+e^- collisions is through the production of the heavier CP-even Higgs boson H either via Higgs-strahlung or in association with A, followed, if kinematically allowed, by the decay $H \to hh$.

In Fig. 4 we plot the relevant cross sections [18,19] for the e^+e^- centre-of-mass energy $\sqrt{s} = 500$ GeV, as functions of the Higgs mass m_H and for $\tan\beta = 2.0$. For a fixed value of m_H, there is seen to be a significant sensitivity to the squark mixing parameters μ and A. We have here taken $\tilde{m} = 1$ TeV, a value which is adopted throughout, except where otherwise specified.

A measurement of the decay rate $H \to hh$ directly yields λ^2_{Hhh}. But this is possible only if the decay is kinematically allowed, and the branching ratio is sizeable (but not too close to unity). In Fig. 5 we show the branching ratios (at $\tan\beta = 2$) for the main decay modes of the heavy CP-even Higgs boson as a function of the H mass [20]. Apart from the hh decay mode, the other important decay modes are $H \to WW^*$, ZZ^*. For increasing values of $\tan\beta$ (but fixed m_h), the Hhh coupling gradually gets weaker (Fig. 1),

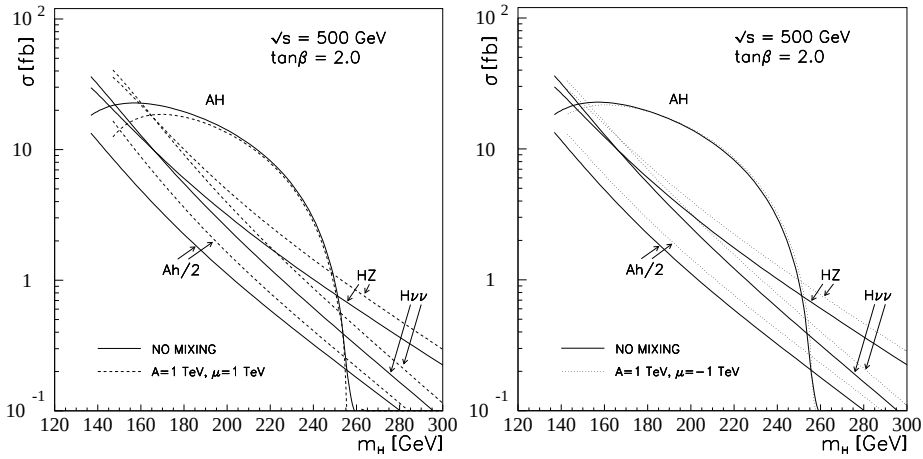

Fig. 4. Cross sections for the production of the heavy Higgs boson H in e^+e^- collisions, and for the background process in which Ah is produced. Solid curves are for no mixing, $A = 0$, $\mu = 0$. Dashed and dotted curves refer to mixing.

and hence the prospects for measuring λ_{Hhh} diminish. Also, the decay rates can change significantly with $\tilde{m}$, the over-all squark mass scale (see Fig. 5).

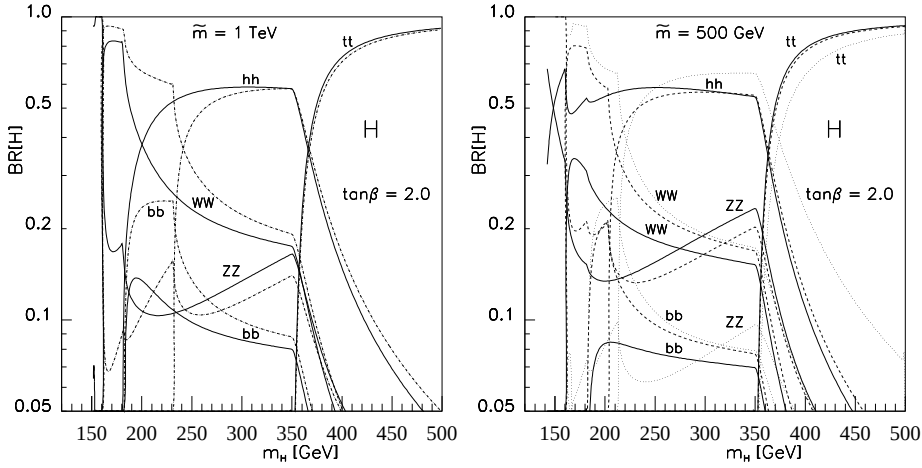

Fig. 5. Branching ratios for the decay modes of the CP-even heavy Higgs boson H, for $\tan\beta = 2.0$ and $\tilde{m}$ equal to 1 TeV or 500 GeV, as indicated. Solid curves are for no mixing, $A = 0$, $\mu = 0$. For $\tilde{m} = 1$ TeV, the dashed curves refer to $A = 1$ TeV and $\mu = 1$ TeV, whereas for $\tilde{m} = 500$ GeV, the dashed (dotted) curves refer to $A = 500$ GeV (800 GeV) and $\mu = 1$ TeV (800 GeV).

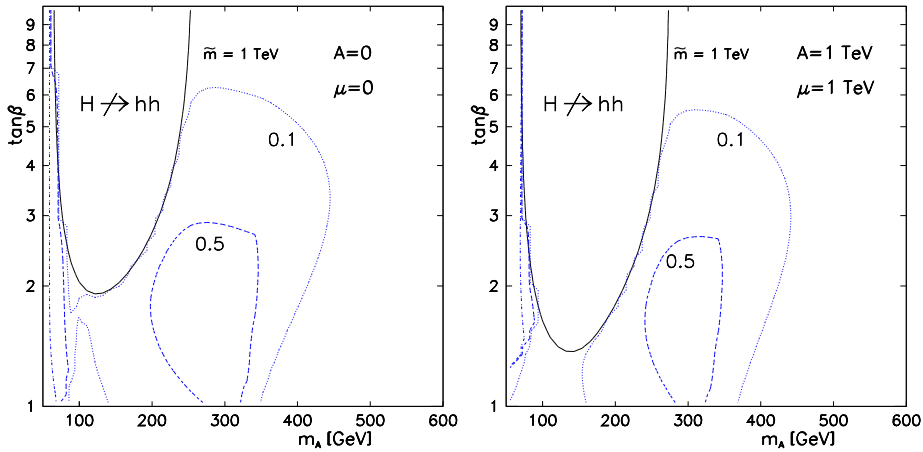

Fig. 6. The region in the m_A–$\tan\beta$ plane where the decay $H \to hh$ is kinematically *forbidden* is indicated by a solid line contour. Also given are contours at which the branching ratio equals 0.1 (dotted), 0.5 (dashed) and 0.9 (dash-dotted, far left).

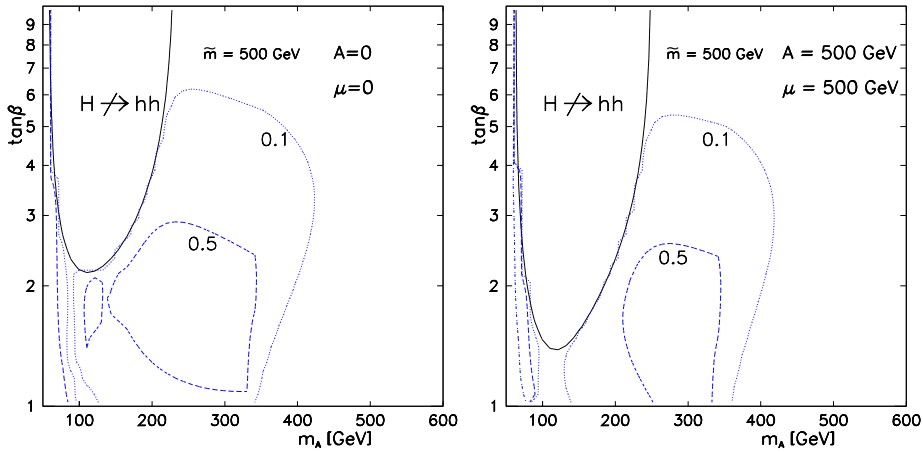

Fig. 7. Similar to Fig. 6, for squark mass parameter $\tilde{m} = 500$ GeV.

There is a sizeable region in the m_A–$\tan\beta$ plane where the decay $H \to hh$ is kinematically forbidden, shown in Figs 6 and 7, as an egg-shaped region at the upper left. The boundary of the region depends crucially on the precise Higgs mass values. This is illustrated by comparing two cases of mixing parameters A and μ at each of two values of the squark mass parameter $\tilde{m}$. We also display the regions where the $H \to hh$ branching ratio is in the range 0.1–0.9. Obviously, in the forbidden region, the λ_{Hhh} cannot be determined from resonant production.

3.2. Double Higgs-strahlung

As discussed above, for small and moderate values of $\tan\beta$, a study of decays of the heavy CP-even Higgs boson H provides a means of determining the triple-Higgs coupling λ_{Hhh}. For the purpose of extracting the coupling λ_{hhh}, non-resonant processes involving two-Higgs (h) final states must be considered. The Zhh final states produced in the non-resonant double Higgs-strahlung $e^+e^- \to Zhh$, and whose cross section involves the coupling λ_{hhh}, could provide one possible opportunity.

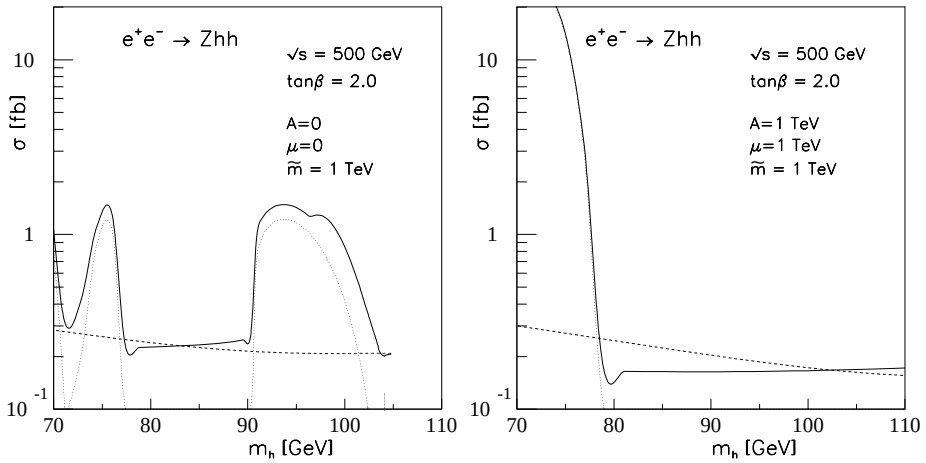

Fig. 8. Cross section $\sigma(e^+e^- \to Zhh)$ as a function of m_h. The dotted curve is the resonant production, the dashed curve gives the decoupling limit [21].

However, the non-resonant contribution to the Zhh cross section is rather small, as is shown in Fig. 8 for $\sqrt{s} = 500$ GeV, $\tan\beta = 2$, and $\tilde{m} = 1$ TeV. In this case, the cross section is rather different for the two sets of mixing parameters shown [4]. In the case of no mixing, there is a broad minimum from $m_h \simeq 78$ to 90 GeV, followed by an enhancement around $m_h \sim 90$–100 GeV. This structure is in part due to the fact that the decay $H \to hh$ is kinematically forbidden in the region $m_h \simeq 78$–90 GeV, see Figs 6 and 7 (this coincides with the opening up of the channel $H \to WW$), followed by an increase of the trilinear couplings.

Since the non-resonant part of the cross section, which depends on λ_{hhh}, is rather small, this channel is not suitable for a determination of λ_{hhh} [3]. In the case of large squark mixing, the cross section can be considerably

larger [4], but only at Higgs masses which are essentially ruled out[1]. At higher values of $\tan\beta$, the cross section is even smaller. For lower values of the squark mass parameter $\tilde{m}$, the cross section can be larger, but again at Higgs masses which are ruled out.

3.3. Fusion mechanism for multiple-h production

A two-Higgs (hh) final state can also result from the WW fusion mechanism in e^+e^- collisions. There is a resonant contribution (through H) and a non-resonant one.

The resonant WW fusion cross section for $e^+e^- \to H\bar{\nu}_e\nu_e$ [23] is plotted in Fig. 4 for the centre-of-mass energy $\sqrt{s} = 500$ GeV, and for $\tan\beta = 2.0$, as a function of m_H.

Besides the resonant WW fusion mechanism for the multiple production of h bosons, there is also a non-resonant WW fusion mechanism:

$$e^+e^- \to \nu_e\bar{\nu}_e hh, \tag{9}$$

through which the same final state of two h bosons can be produced. The cross section for this process (see Fig. 3), can be written in the effective WW approximation as a WW cross section, at invariant energy squared $\hat{s} = xs$, folded with the WW "luminosity" [24]. Thus,

$$\sigma(e^+e^- \to \nu_e\bar{\nu}_e hh) = \int_\tau^1 \mathrm{d}x\, \frac{\mathrm{d}L}{\mathrm{d}x}\, \hat{\sigma}_{WW}(x)\,, \tag{10}$$

where $\tau = 4m_h^2/s$, and

$$\frac{dL(x)}{dx} = \frac{G_\mathrm{F}^2 m_W^4}{2} \left(\frac{1}{2\pi^2}\right)^2 \frac{1}{x}\left\{(1+x)\log\frac{1}{x} - 2(1-x)\right\}. \tag{11}$$

The WW cross section receives contributions from several amplitudes, according to the diagrams (a)–(d) in Fig. 3, only one of which is proportional to λ_{hhh}. We have evaluated these contributions [4], following the approach of Ref. [25], ignoring transverse momenta everywhere except in the W propagators. Our approach also differs from that of [3] in that we do not project out the longitudinal degrees of freedom of the intermediate W bosons.

We show in Fig. 9 the resulting WW fusion cross section, at $\sqrt{s} = 1.5$ TeV, and for $\tilde{m} = 1$ TeV. The structure is reminiscent of Fig. 8, and the

[1] The LEP experiments have obtained strong lower bounds on the mass of the lightest Higgs boson, and are beginning to rule out significant parts of the small-$\tan\beta$ parameter space. ALEPH finds a lower limit of $m_h > 72.2$ GeV, irrespective of $\tan\beta$, and a limit of ~ 88 GeV for $1 < \tan\beta \lesssim 2$ [22].

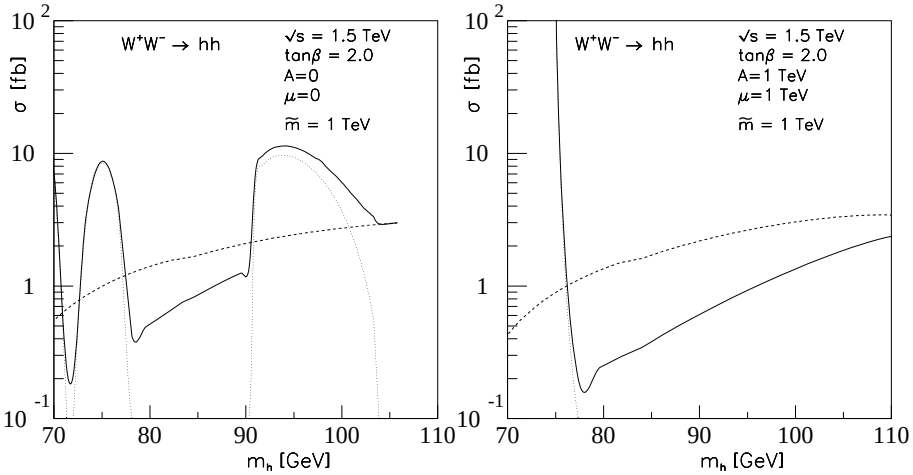

Fig. 9. Cross section $\sigma(e^+e^- \to \nu_e\bar{\nu}_e hh)$ (via WW fusion) as a function of m_h. The dotted curve is the resonant production, the dashed curve gives the decoupling limit.

reasons for this are the same. Notice, however, that the scale is different. Since this is a fusion cross section, it grows logarithmically with energy.

For high values of m_h we see that there is a moderate contribution to the cross section from the non-resonant part. For a lower squark mass scale $\tilde{m}$, the situation is somewhat different. In the absence of mixing, the light Higgs particle then tends to be lighter (for $\tilde{m} = 500$ GeV, $\tan\beta = 2$: $m_h \lesssim 90$ GeV — which is mostly ruled out already [22]). With mixing, however, higher Higgs masses can be reached.

4. Sensitivity to λ_{Hhh} and λ_{hhh}

We are now ready to combine the results and discuss in which parts of the m_A–$\tan\beta$ plane one might hope to measure the trilinear couplings λ_{Hhh} and λ_{hhh}. In Figs 10 and 11 we have identified regions according to the following criteria [3,4]:

(i) Regions where λ_{Hhh} might become measurable are identified as those where $\sigma(H) \times \mathrm{BR}(H \to hh) > 0.1$ fb (solid), while simultaneously $0.1 < \mathrm{BR}(H \to hh) < 0.9$ [see Figs 5–7]. In view of the recent, more optimistic, view on the luminosity that might become available, we also give the corresponding contours for 0.05 fb (dashed) and 0.01 fb (dotted).

(ii) Regions where λ_{hhh} might become measurable are those where the *continuum* $WW \to hh$ cross section [Eq. (10)] is larger than 0.1 fb (solid). Also shown are contours at 0.05 (dashed) and 0.01 fb (dotted).

We have excluded from the plots the region where $m_h < 72.2$ GeV [22]. This corresponds to low values of m_A and low $\tan\beta$. These cross sections

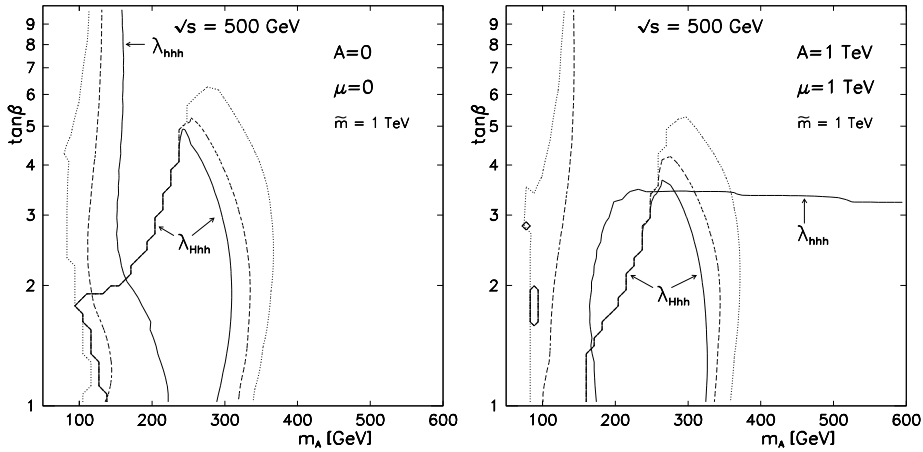

Fig. 10. Regions where trilinear couplings λ_{Hhh} and λ_{hhh} might be measurable at $\sqrt{s} = 500$ GeV. Inside contours labelled λ_{Hhh}, $\sigma(H) \times \mathrm{BR}(H \to hh) > 0.1$ fb (solid), while $0.1 < \mathrm{BR}(H \to hh) < 0.9$. Inside (to the right or below) contour labelled λ_{hhh}, the *continuum* $WW \to hh$ cross section exceeds 0.1 fb (solid). Analogous contours are given for 0.05 (dashed) and 0.01 fb (dotted). Two cases of squark mixing are considered, as indicated.

are small, the measurements are not going to be easy. With an integrated luminosity of 500 fb^{-1}, the contours at 0.1 fb correspond to 50 events per year. This will be reduced by efficiencies, but should indicate the order of magnitude that can be reached.

With increasing luminosity, the region where λ_{Hhh} might be accessible, extends somewhat to higher values of m_A. Note the steep edge around $m_A \simeq 200$ GeV, where increased luminosity does not help. This is determined by the vanishing of $\mathrm{BR}(H \to hh)$, see Figs 6 and 7.

The coupling λ_{hhh} is accessible in a much larger part of this parameter space, but "large" values of $\tan\beta$ are accessible only if A is small, or if the luminosity is high.

The precise region in the $\tan\beta$–m_A plane, in which these couplings might be accessible, depends on details of the model. As a further illustration of this point, we show in Fig. 11 the corresponding plots for a squark mass parameter $\tilde{m} = 500$ GeV. In the case of no mixing, there is now a band at

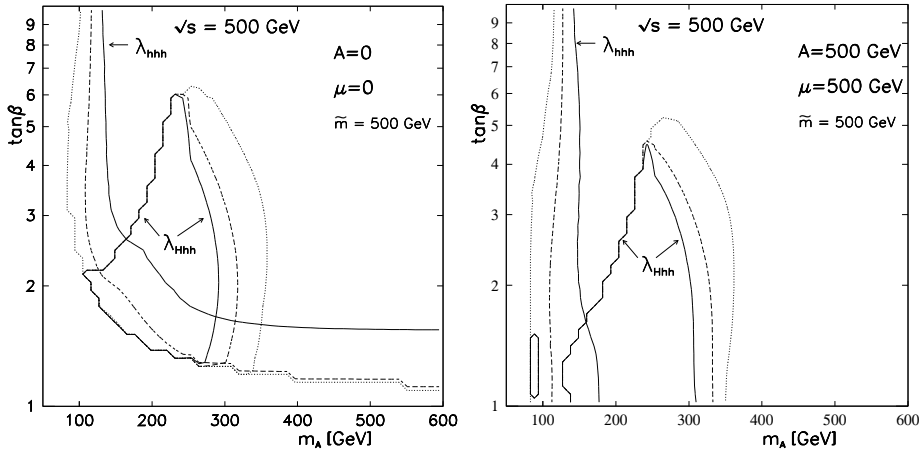

Fig. 11. Similar to Fig. 10 for $\tilde{m} = 500$ GeV.

small m_A and small $\tan\beta$ that is excluded by the Higgs mass bound [22]. Furthermore, where the Higgs mass is low, the coupling λ_{hhh} is small [see Fig. 2], and a corresponding band is excluded from possible measurements.

5. CP studies

In the MSSM, the Higgs sector contains also a particle that is odd under CP. Such particles, as well as Higgs-like particles which are not eigenstates of CP, would be expected in more general electroweak theories. One example would be the two-Higgs-doublet model [6,26]. Model-independent determinations of the Higgs particle CP are possible in the Bjorken process as well as in the electron–electron channel.

There could also be CP violation in the Higgs sector, in which case the Higgs bosons would not be CP eigenstates [27]. Such mixing could take place at the tree level [28], or it could be induced by radiative corrections. It has also been pointed out that such mixing might take place in the MSSM, and be resonant [29].

5.1. The Bjorken process

Certain distributions for the Bjorken process [30] are sensitive to the CP parity. Suitable observables may also demonstrate presence of CP violation.

Below, we present an effective Lagrangian which contains CP violation in the Higgs sector. CP violation usually appears as a one-loop effect, since the CP-odd coupling introduced below is a higher-dimensional operator and in renormalizable models these are induced only at loop level. Thus, the

effects are expected to be small and the confirmation of presence of any CP violation could be rather difficult.

The ZZh coupling is taken to be [9]

$$i2^{5/4}\sqrt{G_F}\begin{cases} m_Z^2\, g^{\mu\nu} & \text{for } h = H \quad \text{(CP even)}, \\ \eta\, \varepsilon^{\mu\nu\rho\sigma} k_{1\rho} k_{2\sigma} & \text{for } h = A \quad \text{(CP odd)}, \end{cases} \tag{12}$$

where k_1 and k_2 are the momenta of the gauge bosons. The CP odd term originates from the dimension-5 operator $\varepsilon^{\mu\nu\rho\sigma} Z_{\mu\nu} Z_{\rho\sigma} H$. Simultaneous presence of CP-even and CP-odd terms leads to CP violation, whereas presence of only the last term describes a pseudoscalar coupling to the vector bosons.

It is well known that the correlation between the two decay planes spanned by the Dalitz pairs from a π^0 decay reveal its pseudoscalar nature [31]. In complete analogy, the orientation of the decay plane spanned by the momenta of the fermions from the Z^0 which is accompanying the Higgs particle in the Bjorken process can be used to determine the CP of the Higgs particle [9–11]. Other methods have also been suggested [7]. These include studies of correlations among momenta of the initial electron and final-state fermions [32].

In fact, a semi-realistic Monte Carlo study shows that (at 300 GeV) it should be possible to verify the scalar character of the Standard Model Higgs after three years of running at a future linear collider [11]. Also, various ways of searching for CP violation have been suggested [9, 11, 33].

5.2. Electron–electron collisions

The electron–electron collider mode is interesting since one may produce states not accessible in the annihilation channel; also, a large electron polarization will be readily available. Furthermore, at high energies, the Higgs production at an electron–electron collider will proceed via gauge boson fusion [34, 35], and thus not be suppressed by the s-channel annihilation mechanism. Certain models also predict doubly charged Higgs particles [36], some of which can be produced more readily at an electron–electron collider.

Scalar ("Higgs") particles, h, h^- and h^{--}, are produced in the t-channel via Z- or W-exchange:

$$e^-(p_1) + e^-(p_2) \;\to\; e^-(p_1') + e^-(p_2') + h(p_h)\,, \tag{13}$$

$$e^-(p_1) + e^-(p_2) \;\to\; e^-(p_1') + \nu_e(p_2') + h^-(p_h)\,, \tag{14}$$

$$e^-(p_1) + e^-(p_2) \;\to\; \nu_e(p_1') + \nu_e(p_2') + h^{--}(p_h)\,. \tag{15}$$

(In some models, including the left–right symmetric model [37], the doubly-charged Higgs boson has practically no coupling to the ordinary, left-handed W bosons and would not be produced by this mechanism.)

Several distributions are quite sensitive to the CP of the Higgs particle. We see immediately from (12) that near the forward direction, where $\boldsymbol{k}_1$ and $\boldsymbol{k}_2$ are antiparallel, the production of a CP-odd Higgs boson will be suppressed.

In the CP-even case, the Higgs particle tends to be softer, and events are more aligned with the beam direction than in the CP-odd case. In fact, the Higgs energy distribution may be one of the better observables for discriminating the two cases, as illustrated in Fig. 12.

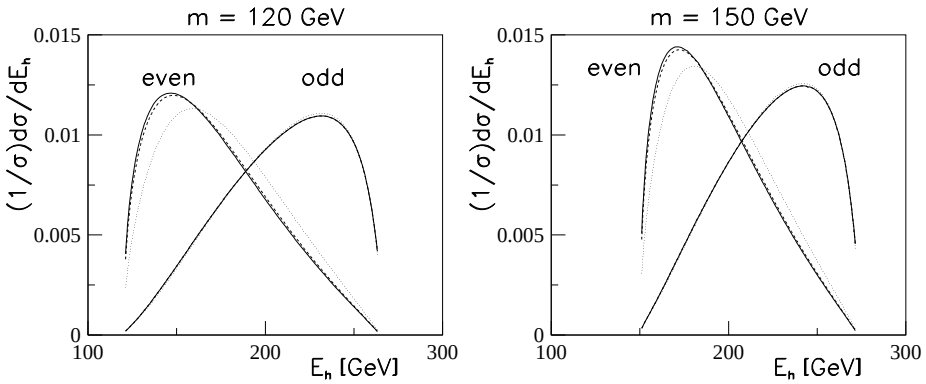

Fig. 12. Higgs energy spectra for the case $E_{\mathrm{c.m.}} = 500$ GeV, and for Higgs masses $m_h = 120$ GeV and 150 GeV. The solid curves give the distributions in the absence of any cut. The dashed and dotted curves show the corresponding distributions when cuts at 5° and 15° are imposed on the electron momenta.

The dependence on longitudinal beam polarization (P_1 and P_2) enters in the following way

$$d^4\sigma^{(h)} = d^4\sigma_0^{(h)} \left[1 + A_1^{(h)}\, P_1 P_2 + A_2^{(h)}(P_1 + P_2)\right]. \tag{16}$$

It turns out that the dependence on the *product* of the two beam polarizations is much larger in the CP-odd case. This dependence, which is represented by the observable A_1 (see Fig. 13), becomes a better "discriminator" for increasing Higgs masses, when the Higgs momentum decreases, and other methods therefore tend to become less efficient.

If the two final-state electrons are observed, a certain azimuthal distribution, as well as the electron polar-angle distributions, will also be useful for discriminating the two cases [12]. There are also ways to search for possible parity-violating effects in the ZZ-Higgs coupling.

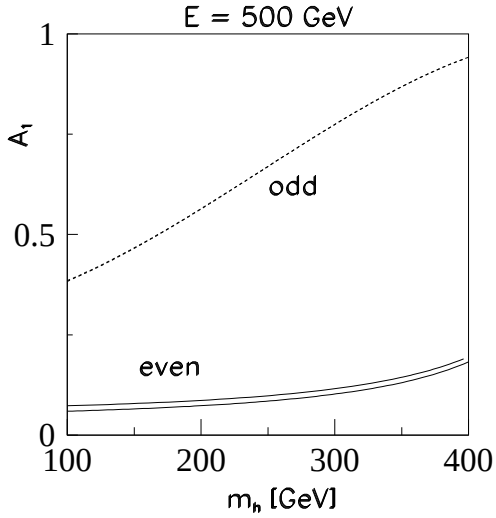

Fig. 13. The bi-polarization-dependence A_1 [see Eq. (16)] as obtained from the integrated cross sections for Higgs production in electron–electron collisions at $E_{\mathrm{c.m.}} = 500$ GeV, for a range of Higgs masses. Standard Model (denoted "even") and CP-odd results are shown. For the even case, the lower curve corresponds to no cut, whereas the upper ones are obtained with an angular cut on the final-state electron momenta at 10°. (For the odd case, the two curves are indistinguishable.)

6. Conclusions

We have reviewed the results of a detailed investigation [4] of the possibility of measuring the MSSM trilinear couplings λ_{Hhh} and λ_{hhh} at an e^+e^- collider, focusing on the importance of mixing in the squark sector, as induced by the trilinear coupling A and the bilinear coupling μ.

At moderate energies ($\sqrt{s} = 500$ GeV) the range in the m_A–$\tan\beta$ plane that is accessible for studying λ_{Hhh} changes quantitatively for non-zero values of the parameters A and μ. As far as the coupling λ_{hhh} is concerned, however, there is a qualitative change from the case of no mixing in the squark sector. If A is large, then high luminosity is required, in order to reach "high" values of $\tan\beta$. At higher energies ($\sqrt{s} = 1.5$ TeV), the mixing parameters A and μ change the accessible region of the parameter space only in a quantitative manner.

We have also given a brief review of some ways to investigate CP properties of the Higgs particles, in e^+e^- as well as in e^-e^- collisions.

This research was supported by the Research Council of Norway. It is a pleasure to thank the organizers of the Epiphany conference for creating a most stimulating meeting. The topics reported on here have been explored with various colleagues whom I would like to thank for stimulating collaborations. Finally, it is with profound gratitude I acknowledge the inspiration that has been provided by Bjørn H. Wiik, whose enthusiasm for basic physics challenges influenced so many of us.

REFERENCES

[1] P. McNamara, invited talk, ICHEP'98, Vancouver 1998, to be published. See also P. M. Zerwas, *Acta Phys. Pol.* **B30**, 1871 (1999).

[2] G. Altarelli, R. Barbieri, F. Caravaglios, *Int. J. Mod. Phys.* **A13**, 1031 (1998).

[3] A. Djouadi, H.E. Haber, P.M. Zerwas, *Phys. Lett.* **B375**, 203 (1996) and Erratum, to be published.

[4] P. Osland, P.N. Pandita, *Phys. Rev.* **D59**, 055013 (1999), and Invited paper, VIIIth UNESCO St. Petersburg International School of Physics, May 25–June 4, 1998. To be published in the Proceedings (Archive: hep-ph/9902270).

[5] A. Djouadi, W. Kilian, M. Muhlleitner, P.M. Zerwas, DESY 99/001 (hep-ph/9903229).

[6] J.F. Gunion, H.E. Haber, G. Kane, S. Dawson, *The Higgs Hunter's Guide*, Addison-Wesley, 1990.

[7] D. Chang, W.Y. Keung, I. Phillips, *Phys. Rev.* **D48**, 3225 (1993); **B329**, 305 (1994); B.A. Kniehl, Proc. Workshop on Physics and Experiments with Linear e^+e^- Colliders, Waikoloa, Hawaii, April 26–30, 1993 vol. II, p. 625; V. Barger, K. Cheung, A. Djouadi, B.A. Kniehl, P.M. Zerwas, *Phys. Rev.* **D49**, 79 (1994); K. Hagiwara, M.L. Stong, *Z. Phys.* **C62**, 99 (1994); M.L. Stong, Invited talk, Ringberg Workshop "Perspectives for Electroweak Interactions in e^+e^- Collisions", Munich, Feb. 5–8, 1995, hep-ph/9504345. M. Krämer, J. Kühn, M.L. Stong, P.M. Zerwas, *Z. Phys.* **C64**, 21 (1994).

[8] E. Accomando *et al., Phys. Rep.* **299**, 1 (1998).

[9] J.R. Dell'Aquila, C.A. Nelson, *Phys. Rev.* **D33**, 101 (1986); D. Chang, W.-Y. Keung, I. Phillips, *Phys. Rev.* **D48**, 3225 (1993).

[10] B. Grządkowski, J.F. Gunion, *Phys. Lett.* **B350**, 218 (1995).

[11] A. Skjold, P. Osland, *Nucl. Phys.* **B453**, 3 (1995).

[12] C.A. Bøe, O.M. Ogreid, P. Osland, Jian-zu Zhang, Bergen Univ. preprint, 1998-09, *Eur. Phys. J.*, **C**, to appear (Archive: hep-ph/9811505).

[13] For reviews, see H.-P. Nilles, *Phys. Rep.* **110**, 1 (1984); H.E. Haber, G.L. Kane, *Phys. Rep.* **C117**, 75 (1985); R. Barbieri, *Riv. Nuovo Cim.* **11**, 1 (1988).

[14] M. Tigner, B. Wiik, F. Willeke, Particle Accel. Conf. IEEE (1991) 2910; S. Kuhlman *et al.* (The NLC ZDR Design Group and the NLC Physics Working Groups), Physics and Technology of the Next Linear Collider: A Report Submitted to Snowmass '96, BNL 52-502, FERMILAB-PUB-96/112, LBNL-PUB-5425, SLAC-Report-485, UCRL-ID-124160, UC-414 (June 1996); H. Murayama, M.E. Peskin, *Ann. Rev. Nucl. Part. Sci.* **46**, 533 (1996); e+e− Linear Colliders: Physics and Detector Studies, R. Settles, editor, Proceedings, workshops, ECFA/DESY, Frascati, London, Munich, Hamburg, DESY-97-123E, 1997.

[15] J. Ellis, G. Ridolfi, F. Zwirner, *Phys. Lett.* **B257**, 83 (1991); *Y. Okada*, M. Yamaguchi, T. Yanagida, *Prog. Theor. Phys.* **85**, 1 (1991); H.E. Haber, R. Hempfling, *Phys. Rev. Lett.* **66**, 1815 (1991); J. Ellis, G. Ridolfi, F. Zwirner, *Phys. Lett.* **B262**, 477 (1991); R. Hempfling, A.H. Hoang, *Phys. Lett.* **B331**, 99 (1994); M. Carena, J.R. Espinosa, M. Quirós, C.E.M. Wagner, Phys. Lett. **B355**, 209 (1995); M. Carena, M. Quirós, C.E.M. Wagner, *Nucl. Phys.* **B461**, 407 (1996); S. Heinemeyer, W. Hollik, G. Weiglein, *Phys. Rev.* **D58**, 091701 (1998).

[16] V. Barger, M.S. Berger, A.L. Stange, R.J.N. Phillips, *Phys. Rev.* **D45**, 4128 (1992).

[17] A. Sirlin, R. Zucchini, *Nucl. Phys.* **B266**, 389 (1986).

[18] G. Pócsik, G. Zsigmond, *Z. Phys.* **C10**, 367 (1981).

[19] J.F. Gunion, L. Roszkowski, A. Turski, H.E. Haber, G. Gamberini, B. Kayser, S.F. Novaes, F. Olness, J. Wudka, *Phys. Rev.* **D38**, 3444 (1988).

[20] For a review, see A. Djouadi, J. Kalinowski, P.M. Zerwas, *Z. Phys.* **C70**, 435 (1996).

[21] H.E. Haber, in Proceedings of the Conference on *Perspectives for Electroweak Interactions in e^+ e^- Collisions*, Ringberg (Tegernsee), Germany, 1995; ed. B.A. Kniehl, World Scientific, Singapore 1995, p. 219.

[22] R. Barate *et al.* (ALEPH Collaboration), *Phys. Lett.* **B440**, 419 (1998).

[23] A. Djouadi, D. Haidt, B.A. Kniehl, B. Mele, P.M. Zerwas, in Proceedings, Workshop on e^+e^- Collisions at 500 GeV: The Physics Potential, Munich-Annecy-Hamburg (DESY 92-123 A, Hamburg, 1992).

[24] R.N. Cahn, S. Dawson, *Phys. Lett.* **B136**, 196 (1984); S. Dawson, *Nucl. Phys.* **B249**, 42 (1984); M. Chanowitz, M.K. Gaillard, *Phys. Lett.* **B142**, 85 (1984); I. Kuss, H. Spiesberger, *Phys. Rev.* **D53**, 6078 (1996).

[25] G. Altarelli, B. Mele, F. Pitolli, *Nucl. Phys.* **B287**, 205 (1987).

[26] T.D. Lee, *Phys. Rev.* **D8**, 1226 (1973).

[27] For a recent review, see, W. Bernreuther, Lectures given at 37th Internationale Universitätswochen für Kernphysik und Teilchenphysik, Schladming, Austria, 28 Feb - 7 Mar 1998; hep-ph/9808453.

[28] N.G. Deshpande, E. Ma, *Phys. Rev.* **D16**, 1583 (1977); M. Matsuda, M. Tanimoto, *Phys. Rev.* **D52**, 3100 (1995).

[29] A. Pilaftsis, *Phys. Rev. Lett.* **77**, 4996 (1996); *Nucl. Phys.* **B504**, 61 (1997); *Phys. Lett.* **B435**, 88 (1998).

[30] J. D. Bjorken, in Proceedings of the 1976 SLAC Summer Institute on Particle Physics, ed. M. Zipf (SLAC Report No. 198, 1976) p. 22; B.L. Ioffe, V.A. Khoze, *Sov. J. Part. Nucl.* **9**, 50 (1978); D.R.T. Jones, S.T. Petcov, *Phys. Lett.* **84B**, 440 (1979); J. Finjord, *Phys. Scr.* **21**, 143 (1980).

[31] C.N. Yang, *Phys. Rev.* **77**, 242, 722 (1950); N. Kroll, W. Wada, *Phys. Rev.* **98**, 1355 (1955); R.H. Dalitz, *Proc. Phys. Soc.* (London) **A64**, 667 (1951).

[32] T. Arens, U.D.J. Gieseler, L.M. Sehgal, *Phys. Lett.* **B339**, 127 (1994); T. Arens, L.M. Sehgal, *Z. Phys.* **C66**, 89 (1995).

[33] A. Djouadi, B.A. Kniehl, in Proceedings of the Workshop on e^+e^- Collisions at 500 GeV: The Physics Potential, Munich, Annecy, Hamburg, 1992/93, edited by P.M. Zerwas, DESY Report No. DESY 93–123C, pp. 51–54; K. Hagiwara, M.L. Stong, *Z. Phys.* **C62**, 99 (1994); M.L. Stong, Invited talk, Ringberg Workshop Perspectives for Electroweak Interactions in e^+e^- Collisions, Munich, Feb. 5–8, 1995, hep-ph/9504345; J.R. Dell'Aquila, C.A. Nelson, *Nucl. Phys.* **B320**, 61, 86 (1989).

[34] K.I. Hikasa, *Phys. Lett.* **B164**, 385 (1985); Err. *Phys. Lett.* **B195**, 623 (1987).

[35] V. Barger, J.F. Beacom, Kingman Cheung, T. Han, *Phys. Rev.* **D50**, 6704 (1994); T. Han, *Int. J. Mod. Phys.* **A11**, 1541 (1996); P. Minkowski, *Int. J. Mod. Phys.* **A13**, 2255 (1998).

[36] H. Georgi, M. Machacek, *Nucl. Phys.* **B262**, 463 (1985); R. Vega, D.A. Dicus, *Nucl. Phys.* **B329**, 533 (1990); J.F. Gunion, R. Vega, J. Wudka, *Phys. Rev.* **D42**, 1673 (1990).

[37] J.C. Pati, A. Salam, *Phys. Rev.* **D10**, 275 (1974); R.N. Mohapatra, J.C. Pati, *Phys. Rev.* **D11**, 566 (1975); G. Senjanovic, R.N. Mohapatra, *Phys. Rev.* **D12**, 1502 (1975); R.E. Marshak, R.N. Mohapatra, *Phys. Lett.* **91B**, 222 (1980).